



Mild alkaline separation of fiber bundles from eucalyptus bark and their composites with cellulose acetate butyrate

Jinze Dou^{a,*}, Alp Karakoç^{a,b}, Leena-Sisko Johansson^a, Sami Hietala^c, Dmitry Evtuygin^d, Tapani Vuorinen^{a,*}

^a Department of Bioproducts and Biosystems, School of Chemical Engineering, Aalto University, Vuorimiehentie 1, P.O. Box 16300, 00076, Aalto, Finland

^b Department of Communications and Networking, School of Electrical Engineering, Aalto University, Maarintie 8, P.O. Box 13000, 00076, Aalto, Finland

^c Department of Chemistry, University of Helsinki, P.O. Box 55, FI-00014, Finland

^d CICECO/Department of Chemistry, University of Aveiro, 3810-193, Aveiro, Portugal

ARTICLE INFO

Keywords:

Eucalyptus bark
Biodegradable
Cellulose ester
Composite
Fiber bundle

ABSTRACT

High surface lignin content (i.e. 34.6 %) sclerenchyma fiber bundles were successfully isolated with a yield of 71 % by a mild alkali (NaOH dosage of 5 wt%) extraction of eucalyptus (*Eucalyptus globulus*) bark under 100 °C for 60 min.. The mechanical properties of the composites prepared by hot pressing of cellulose acetate butyrate (CAB) sheets with the fiber bundles were evaluated. The fiber bundles exhibited good compatibility with CAB due to their hydrophobic fiber surfaces. The mechanical properties of the fiber bundle/ cellulose acetate butyrate composites revealed the maximum at a weight ratio of 25:75, which demonstrates the promise of utilizing these isotropic aligned fiber bundles as the reinforcement to the cellulose acetate butyrate without the addition of plasticizers for composite uses.

1. Introduction

The concept of ‘the bark biorefinery’ (Normand et al., 2014; Dou et al., 2016) is envisioned to produce the value-added bio-products by utilizing the discarded substances of the bark from the forest industry, which can contribute by decreasing the carbon footprint of the earth, benefitting the forest land owners and increasing the profitability of the pulp producers and paper packaging industries. (Devappa et al., 2015; Neis et al., 2019)

Commercially, the eucalyptus *spp.* tree species are cultivated as fast-growing crops, and have been utilized as the key source for pulp and paper industry from countries like Australia, Portugal (Águas et al., 2017), Brazil (Elli et al., 2020), and China (Xie et al., 2017). The bark represents more than 11 % of the volume of the stem depending on the harvesting sites, tree age and hybrid variations. (Quilhó and Pereira, 2001) Additionally, as the bark shedding is a remarkable feature for the eucalyptus, the external layer of the bark is seasonally stripped off to keep the trees healthy. (Chattaway, 1955) Such fallen bark has been also considered as a threat for creating fire hazard in the forest. (Grootemaat et al., 2017) Furthermore, the bark volumes can increase because of the negative health effect on the use of methyl bromide (Park et al., 2020)

that has been used for fumigation purposes, which also means that only the de-barked wood are allowed to be exported to other countries. The bark has been conventionally used for energy production but not for wood pulp production because of bark’s high content of phenolics and other extractives hindering the pulping process. (Miranda et al., 2012) More attention has been paid on the delignification of *Eucalyptus* wood using green solvents (such as deep eutectic solvents) under milder conditions. (Soares et al., 2021) Studies on the bioactivities of the eucalyptus extracts have been carried out previously at the bark (Fernández et al., 2019; Vázquez et al., 2008) and leaves (Pan et al., 2020; Yong et al., 2019), while quite little is known about the separation and further usage of its sclerenchyma fiber bundles (FBs).

Non-woody lignocellulosic derived fibers (or bundles) are used as reinforcement materials for composites due to their high aspect ratio, biodegradability, and low cost. (Dou et al., 2019; Pickering et al., 2016) However, the overall mechanical properties of the composite are always compromised due to the poor compatibility between fiber and matrix. (Saha et al., 2016) Therefore, compatibilization strategies (e.g. the use of coupling or sizing agents) can improve the accessibility of the polymer matrixes through surface modification. (Saha et al., 2016) Alkali-pretreatment has also been reported to enhance the fiber-matrix

* Corresponding authors. Present address: Vuorimiehentie 1, Espoo, Finland.

E-mail addresses: jinze.dou@aalto.fi (J. Dou), tapani.vuorinen@aalto.fi (T. Vuorinen).

<https://doi.org/10.1016/j.indcrop.2021.113436>

Received 30 October 2020; Received in revised form 9 March 2021; Accepted 15 March 2021

Available online 23 March 2021

0926-6690/© 2021 The Author(s).

Published by Elsevier B.V. This is an open access article under the CC BY-NC-ND license

(<http://creativecommons.org/licenses/by-nc-nd/4.0/>).



Fig. 1. Experimental flow of fiber bundle separation from eucalyptus bark under mild alkaline conditions and preparation of fiber bundle composites.

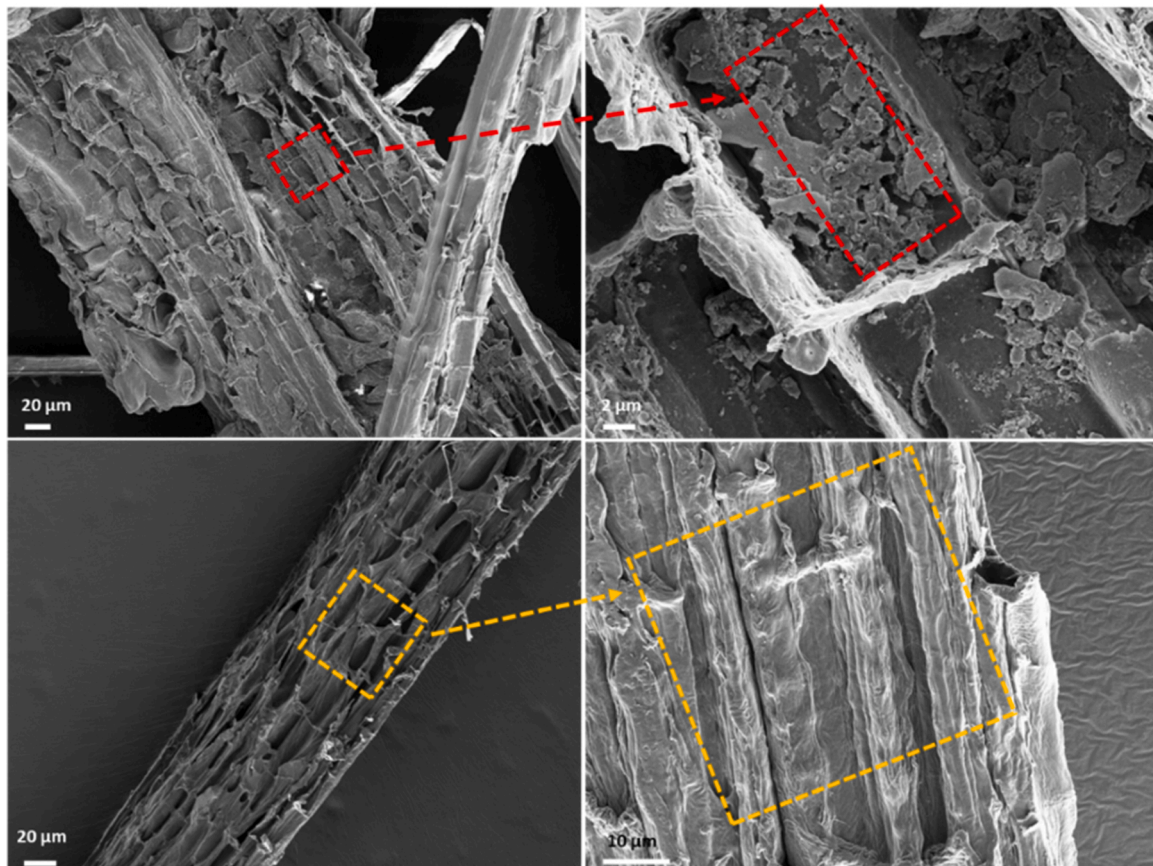


Fig. 2. SEM images of Eucalyptus bark fiber bundle complexes with individual fiber bundles. Upper images refer to the fiber bundle association, especially the scattered fragments that are possibly associated to the parenchyma cells; Bottom images refer to the individual fiber bundle.

interfacial adhesion, thus maximizing the mechanical performance of the composites. (Mazzanti et al., 2019)

Cellulose acetate butyrate (CAB), has been seen as one of the common commercial cellulose ester derivatives that is actually comparable with the composites that made from the polypropylene. (Oujai and Shanks, 2009) Thus, Wibowo et al. also demonstrates that with longer butyrate branch from CAB provides better flexural strength and elastic

characteristics than the cellulose acetate although both of them require the usage of plasticizer for lowering down the glass transition temperature and improving the flexibility of composites. (Wibowo et al., 2004) The aim of the study is thus to investigate the possibilities of separating the sclerenchyma fiber bundles by a mild alkali treatment and their use as the reinforcement to the CAB matrix.

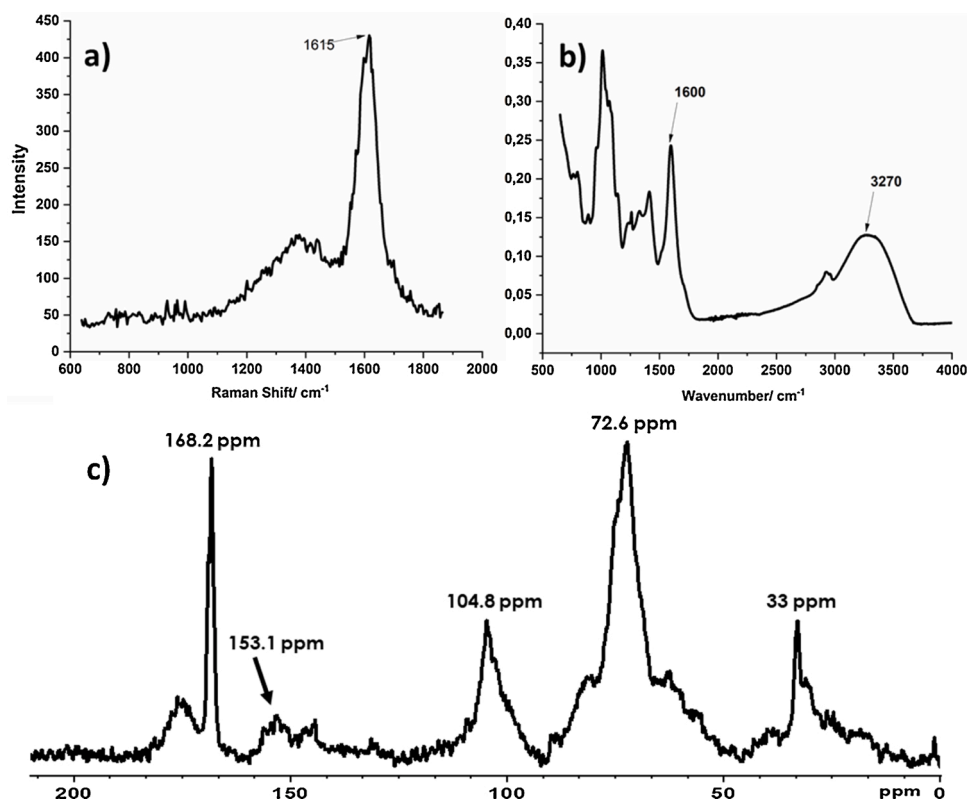


Fig. 3. Structural characterization of the lyophilized high molecular weight fractions (liquid fraction) that were collected after dialysis of the liquid from 5 % NaOH treatment of eucalyptus bark: a) UVRR spectrum; b) IR spectrum; c) ^{13}C CP/MAS NMR spectrum.

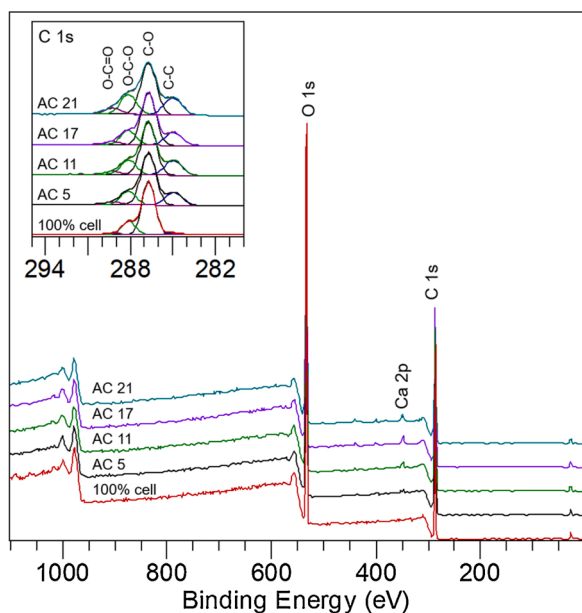


Fig. 4. XPS spectra of acetone extracted eucalyptus bark fiber bundles. Nominal surface coverage of lignins, calculated from the C 1s component of C-C at 285 eV, ranged from 28.9 % to 34.6 %.

2. Materials and methods

2.1. Plant material and chemicals

Bark from eucalypt wood (*Eucalyptus globulus*) were obtained from industrial stem debarking in pulp mills in Portugal (Navigator Comp.,

Industrial complex of Aveiro), air dried in dark place and stored at 20 °C for further investigations. The cellulose acetate butyrate (CAB-500-5) was supplied by Eastman Chemical Company. The screener used to collect the fiber bundles was from IKEA. The sodium hydroxide pellets (NaOH) was purchased from VWR. (–)-Epicatechin, arabinose, rhamnose, galactose and xylan were supplied by Sigma-Aldrich.

2.2. Methods

As visualized in Fig. 1, hot water extraction was applied to extract the hydrophilic substances under 80 °C for 20 min (liquid to bark ratio is 20:1). The hot water extracts were freeze-dried for further analysis. Then, alkali treatment (AT) was applied in a silicon oil-bath heated iron container (Haatuote, model 43427) at 100 °C for 60 min with the loads of NaOH ranging from 5 to 23 % (w/w). Thereafter, filtration was applied to separate the diluted spent liquor (liquid phase) and the fiber bundles (solid phase). The liquid fraction was further dialyzed (>6–8 kDa), centrifuged and lyophilized to obtain the high molecular weight (HMW) fractions for additional analysis. The separated fiber bundles were washed and further disintegrated with a mechanical mixer to separate the sclerenchyma fiber bundles from their flocs. The fiber bundle sheets were fabricated using the Lorentzen & Wettre (L&W) hand sheet mold before drying under the L&W drum dryer at the drum surface temperature of 65 °C. The fiber bundles and the CAB matrix were kept at room temperature for reaching the equilibrium conditions (ca. 60 % relative humidity). The composites were further assembled by placing the fiber bundle sheet in between the evenly pre-weighted CAB layers. Finally, the composite was prepared by hot pressing the laminated structure at 205 °C for 2 min under the pressure of 9.8 bar, as shown in Fig. 1.

The microstructure of composites was assessed by scanning electron microscopy (SEM) that was carried out using a Zeiss Sigma VP operating at 4 kV. The fiber bundle fragments and the topographies of the tensile

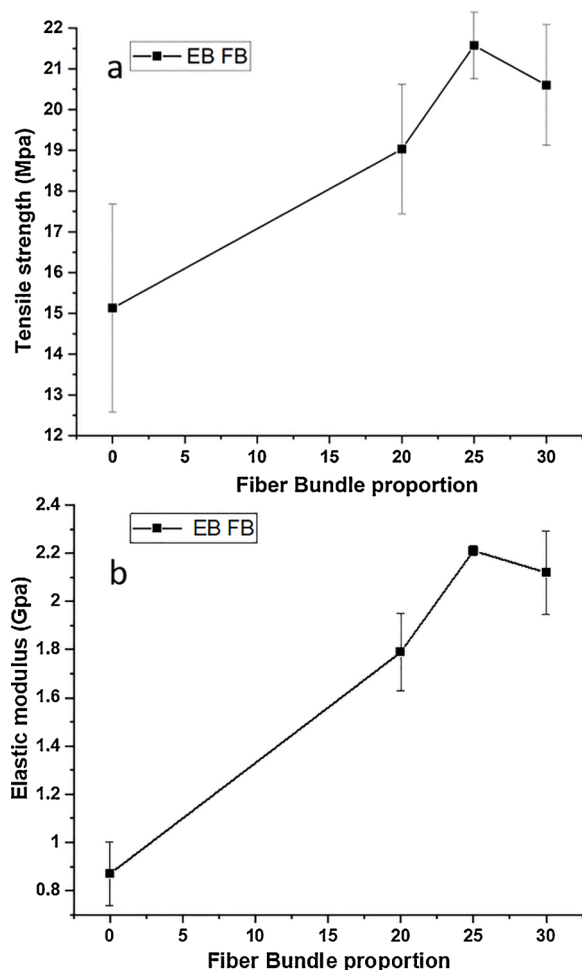


Fig. 5. Plots of tensile strength (a) and elastic modulus (b) as a function of fiber bundle's proportion from eucalyptus bark.

Table 1
Density and tensile properties of the composites^a.

	FBO CAB 100	FB 20 CAB 80	FB 25 CAB 75	FB 30 CAB 70
Density (g/cm ³)	0.86	1.03	1.00	0.97
Grammage (g/m ²)	593.3 (74)	885.0 (20)	803.6 (26)	761.5 (41)
Tensile strength (MPa)	15.13 (2.55)	19.03 (1.59)	21.57 (0.82)	20.60 (1.48)
Tensile index (KN m kg ⁻¹)	17.48 (1.97)	18.56 (1.29)	21.49 (1.58)	21.21 (1.12)
Breaking strain (%)	3.65 (0.54)	1.82 (0.07)	1.61 (0.32)	1.46 (0.16)
Elastic modulus (GPa)	0.87 (0.13)	1.79 (0.16)	2.21 (0.02)	2.12 (0.17)
Specific elastic modulus (MN m kg ⁻¹)	1.00 (0.15)	1.74 (0.16)	2.21 (0.02)	2.18 (0.18)

^a FBxx CAB yy with xx refers to the fiber bundle content (% w/w); yy refers to the content of the CAB matrix.

fractured surfaces from the fiber bundle composites were sputter-coated with the Platinum/palladium (Pt/Pd) for ensuring its electronic conductivity. Solid-state CP/MAS ¹³C NMR spectra were registered on a Bruker Avance III spectrometer operating at 500 MHz for protons using a double resonance CP/MAS probe head. Samples were packed into 4 mm o.d. ZrO₂ rotors plugged with KEL-F® endcaps and spun at spinning frequency of 8 kHz. The length of the contact time for cross polarization was 1 ms and a variable amplitude cross polarization ramped from 70 %

to a maximum amplitude during contact time was used. During the acquisition period the protons were decoupled using SPINAL-64 decoupling and the length of the acquisition was 27 ms. At least 3000 scans were collected with a 5 s relaxation delay and spectra externally referenced to adamantane. All the NMR spectra were processed using TopSpin 4.0 software.

Tensile testing was conducted using the MTS 400/M Vertical Tensile Tester (12 mm min⁻¹ cross-head speed, 2 kN load cell and 100 mm clamp span). The composite specimen size is 15 mm wide and 130 mm length. The tensile strength, tensile index, breaking strain, and elastic modulus were calculated from the stress-strain curves. An average of seven specimens were independently tested. An average thickness of 0.78 mm was achieved.

The surface lignin content of the fiber bundles was evaluated by X-ray photoelectron spectroscopy (XPS), as described previously. (Dou et al., 2019) The carbohydrate and the lignin contents of the eucalyptus bark (EB), hot water extracted eucalyptus bark (HWE EB) and EB FBs were characterized by following the standard procedures (NREL/TP-510-42618). (Sluiter et al., 2010) The sugars analysis was performed using a high-performance anion-exchange chromatography (HPAEC) with pulsed amperometric detection (PAD) (Dionex ICS-3000, CarboPac PA20 column, Sunnyvale, CA, USA). Additionally, ultraviolet resonance Raman (UVR) and infrared (IR) spectroscopy were used to analyze the chemical structure of the HMW fractions as described previously. (Dou et al., 2018a)

3. Results and discussions

3.1. Hot water extracts and fiber bundle separation

Hydrophilic extracts (HWE) were obtained with a yield of 4.7 % based on the starting material of the eucalyptus bark, which is comparable with that of the previously published data. (Fernández et al., 2019; Neiva et al., 2020) In addition, approximately 70 % (-)-epicatechin equivalent phenols demonstrate the promise of being further utilized as natural sources of antioxidants (Table S1 and Fig. S1-S3, supporting information). (Vázquez et al., 2008, 2012) The monomeric sugars of the HWE increased after the acid treatment through the hydrolysis of the glucosides (the content increased from 8 mg/g to 116 mg/g), and the main monomeric sugars after acid treatment were glucose and mannose as shown in Fig. S4, whereas fructose disappeared after the acid treatment.

Even though Eucalyptus bark (EB) contains longer sclerenchyma fibers than its wood section (Jorge et al., 2000), this will require higher pulping strength to separate the fibers as EB lignin (Neiva et al., 2020) contains less reactive syringyl-type lignin (Li et al., 2003; Shimizu et al., 2012) than its corresponding wood section (Rencoret et al., 2011), a similar difference has been observed in willow (Dou et al., 2018b). Therefore, the target was set to develop a simple and industrially scalable method for separating the sclerenchyma fiber bundles (Dou et al., 2019, 2021b) rather than individual fibers from EB. Table S2 illustrates the effect of the NaOH loads to the extract yield of the separated fiber bundles. It shows the fiber bundle separation can be achieved under the lowest NaOH dosage of 5 % with the yield of 71 %. The fiber bundle association and the well-separated fiber bundles can be observed in the scanning electron microscopy (SEM) images shown in Fig. 2. Another remarkable observation is the presence of the scattered fragments that is associated to some remaining of parenchyma cells, which was also referred in the literature (Lima et al., 2013).

3.2. Characterization of the lyophilized high molecular weight hydrolysates

Infrared (IR) and ultraviolet resonance Raman (UVR) spectra of the HMW fractions (Fig. 3) revealed a strong band near 1605 cm⁻¹ (1615 and 1600 cm⁻¹ for UVR and IR, respectively) assigned to the skeletal

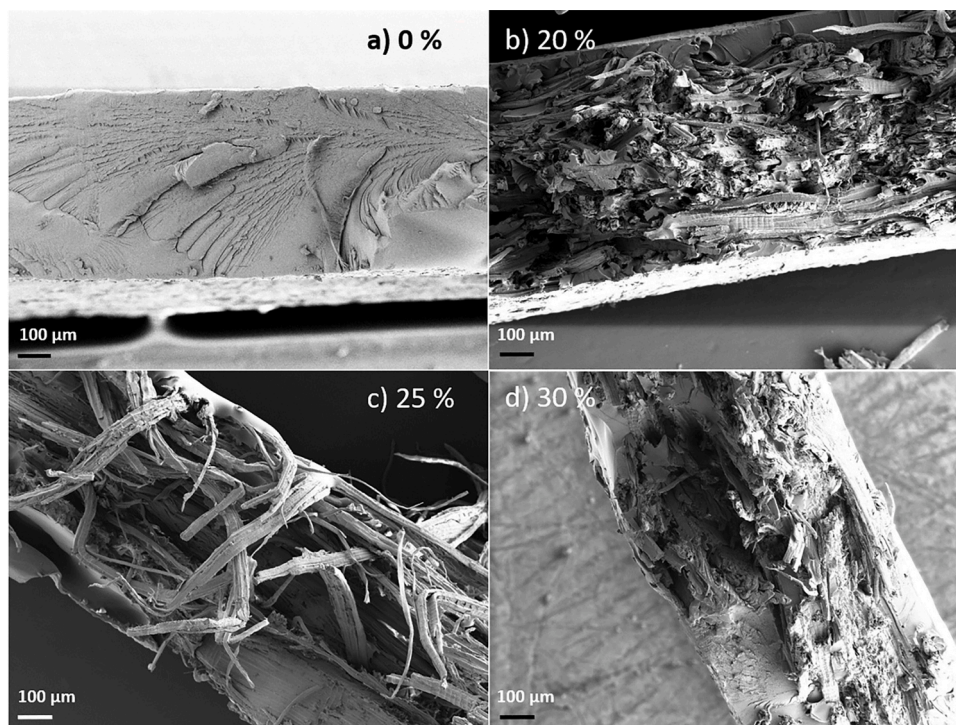


Fig. 6. SEM images of the tensile fractured surfaces from the fiber bundle composites together with the original cellulose acetate butyrate: a) FB 0 CAB 100; b) FB 20 CAB 80; c) FB 25 CAB 75; d) FB 30 CAB 70. FB xx CAB yy with xx refers to the fiber bundle content (% w/w); yy refers to the content of the CAB matrix.

vibrations in aromatic rings. Additionally, the CP/MAS ^{13}C NMR spectrum showed high signal intensities for carboxylic acid $\text{C}=\text{O}$ groups (168.2 ppm), the $\text{O}-\text{CH}_2$ methylene adjacent to ester groups (72.6 ppm) and the methylene linkages (33 ppm). The eventual presence of polysaccharides may be suggested considering the C1 signal of hemicelluloses at 104.8 ppm. Additionally, **Fig. S5** and **Table S3** demonstrated the disappearance of the aliphatic methyl groups (21.4 ppm) from the original EB that reappeared at 33 ppm in HMW fractions. (**Kono et al., 2002**) **Fig. S6** also shows the residual lignin content was ca. 20.4 % in comparison with 25.1 % and 25.6 % Klason lignin content from the original eucalyptus bark and hot water extracted bark, respectively. Therefore, it can be inferred that the HMW fractions did not represent essentially lignin but possibly the majority of the material originated from suberin and hemicelluloses, which is in agreement with the findings that hemicelluloses can be relatively easily solubilized under low alkali environments (**Lima et al., 2013**). The recovered hemicellulose can be catalytically valorized into production of furfural (**Dulie et al., 2021**), which is beyond the scope of this study.

3.3. Hydrophobicity of the fiber bundles and their composite use

The surface chemical composition of the FBs was studied by X-ray photoelectron spectroscopy (XPS) (**Johansson et al., 2004**) to determine the nominal surface lignin coverage of the acetone extracted samples. The nominal lignin surface coverage ranged from 28.9%–34.6% on the selected samples from NaOH dosages of 5, 11, 17 and 21 %, as shown in **Fig. 4**, **Table S4** and **Fig. S7**.

The composite use of FBs was motivated by their high surface lignin content (i.e. 34.6 %) that might be beneficial for achieving high compatibility with a hydrophobic polymer. As can be seen from **Fig. 5**, **Table 1** and **Fig. S8**, the FB (with the highest fiber surface lignin coverage)/CAB composites yielded the maximal increase in elastic modulus and tensile strength at the FB/CAB weight ratio of 25:75. However, higher FB proportion (>25 %) resulted in detrimental effect on the fiber matrix contact and promoted the increase of voids since the FB started to aggregate as it shown in **Fig. 6**. The density trend with

increasing fiber content tabulated in **Table 1** clearly reveals the existence of voids inside the composites, i.e. 1.00 g/cm^3 for FB 25 CAB 75 while 0.97 g/cm^3 for FB 30 CAB 70. In addition, FB aggregation behavior hindered the CAB penetration inside the fiber bundles. Although fibers were intact, the lack of CAB reduced the load transfer among the fibers. The fiber aggregation and matrix penetration issues have been also observed in various bio-based composite studies and previously documented in the literature (**Karakoç et al., 2020**; **Sajaniemi et al., 2019**; **Ku et al., 2011**). Especially, this is obvious for the strength and strain at break (see the related values at **Table 1** and **Fig. S8**) since the weak fiber-matrix contact and voids results as poor matrix penetrations inside the fiber aggregate and act as the load hindering components for the composite after the yield point.

On the other hand, FB/CAB composites can reach up to higher fiber contents, where the optimal content value is between 25–30 % resulting in stiffness and tensile strength increases of 144 % and 43 %, respectively. Although these values are promising in consideration to their contributions to the stiffness and strength, there are still many rooms for improvement concerning the fiber treatment, impregnation and inter-phase compatibility, which can provide higher optimal fiber content values with increasing mechanical characteristics.

4. Conclusions

The present study reveals that the fiber bundles from eucalyptus bark can be effectively separated under low alkalinity conditions at temperatures below 100°C . The high lignin content on the fiber surface made the fiber bundle surface relatively compatible with the matrix of the cellulose acetate butyrate. Additionally, the cellulose acetate butyrate proves to be a suitable thermoplastic biodegradable polymer that can be substantially reinforced by the naturally isolated fiber bundles from eucalyptus bark without the addition of plasticizers. Moreover, this is also first time demonstrating the fiber bundle separation that can be integrated with the usage of the valuable hot water extracts (**Dou et al., 2021a**) from the discarded eucalyptus bark. Further efforts are still needed to reveal the antioxidant activity and its specific phytochemical

contents of the hot water extracts from eucalyptus bark.

The study also shows that the strength and stiffness of the plant-based fiber polymer composites is highly influenced by the fiber loading. It was observed that the mechanical properties increased with the fiber content up to an optimal value, which is around 25–30 %. Above this content, load distribution was not anymore uniform among the fibers due to lack of matrix and fiber bonding and existing voids because of insufficient impregnation. This shows that there is still space to improve for the fiber surface treatment and impregnation, which can result in better bonding and load transfer between the fiber bundles.

CRedit authorship contribution statement

Jinze Dou: Conceptualization, Methodology, Validation, Formal analysis, Investigation, Resources, Writing - original draft, Supervision. **Alp Karakoç:** Formal analysis, Investigation, Writing - review & editing. **Leena-Sisko Johansson:** Formal analysis, Investigation. **Sami Hietala:** Investigation, Writing - review & editing. **Dmitry Evtyugin:** Resources, Writing - review & editing. **Tapani Vuorinen:** Conceptualization, Methodology, Project administration, Supervision, Writing - review & editing.

Declaration of Competing Interest

The authors declare that they have no known competing financial interests or personal relationships that could have appeared to influence the work reported in this paper.

Acknowledgements

This work made use of the Aalto University Nanomicroscopy Center (Aalto-NMC) premises. The authors thank Rita Hatakka from Aalto University for her skillful assistance in HPAEC measurement. This work was a part of the Academy of Finland's Flagship Programme under Projects No. 318890 and 318891 (Competence Center for Materials Bioeconomy, FinnCERES). Authors thank RAIZ (Portuguese Research Institute on Forestry and Paper) for supplying the eucalyptus bark sample used within the scope of the project Impactus – innovative products and technologies from eucalyptus, Project N.º 21874 funded by Portugal 2020 through European Regional Development Fund (ERDF) in the frame of COMPETE 2020 nº246/AXIS II/2017.

Appendix A. Supplementary data

Supplementary material related to this article can be found, in the online version, at doi:<https://doi.org/10.1016/j.indcrop.2021.113436>.

References

- Águas, A., Larcombe, M.J., Matias, H., Deus, E., Potts, B.M., Rego, F.C., Silva, J.S., 2017. Understanding the naturalization of *Eucalyptus globulus* in Portugal: a comparison with Australian plantations. *Eur. J. For. Res.* 136, 433–446. <https://doi.org/10.1007/s10342-017-1043-6>.
- Chattaway, M.M., 1955. The anatomy of bark. V. *Eucalyptus* species with stringy bark. *Aust. J. Bot.* 3, 165–169. <https://doi.org/10.1071/BT9550165>.
- Devappa, R.K., Rakshit, S.K., Dekker, R.F.H., 2015. Forest biorefinery: potential of poplar phytochemicals as value-added co-products. *Biotechnol. Adv.* 33, 681–716. <https://doi.org/10.1016/j.biotechadv.2015.02.012>.
- Dou, J., Galvis, L., Holopainen-Mantila, U., Reza, M., Tamminen, T., Vuorinen, T., 2016. Morphology and overall chemical characterization of willow (*Salix* sp.) inner bark and wood: toward controlled deconstruction of willow biomass. *ACS Sustainable Chem. Eng.* 4, 3871–3876. <https://doi.org/10.1021/acsschemeng.6b00641>.
- Dou, J., Xu, W., Koivisto, J.J., Mobley, J.K., Padmakshan, D., Kögler, M., Xu, C., Willför, S., Ralph, J., Vuorinen, T., 2018a. Characteristics of hot water extracts from the bark of cultivated willow (*Salix* sp.). *ACS Sustainable Chem. Eng.* 6, 5566–5573. <https://doi.org/10.1021/acsschemeng.8b00498>.
- Dou, J., Kim, H., Li, Y., Padmakshan, D., Yue, F., Ralph, J., Vuorinen, T., 2018b. Structural characterization of lignins from willow bark and wood. *J. Agric. Food Chem.* 66, 7294–7300. <https://doi.org/10.1021/acs.jafc.8b02014>.
- Dou, J., Paltakari, J., Johansson, L.-S., Vuorinen, T., 2019. Novel insight into the separation and composite utilization of sclerenchyma Fiber bundles of willow bark.

- ACS Sustain. Chem. Eng. 7, 2964–2970. <https://doi.org/10.1021/acsschemeng.8b04001>.
- Dou, J., Heinonen, J., Vuorinen, T., Xu, C., Sainio, T., 2021a. Chromatographic recovery and purification of natural phytochemicals from underappreciated willow bark water extracts. *Sep. Purif. Technol.* 261, 118247. <https://doi.org/10.1016/j.seppur.2020.118247>.
- Dou, J., Rissanen, M., Ilina, P., Mäkkylä, H., Tammela, P., Haslinger, S., Vuorinen, T., 2021b. Separation of fiber bundles from willow bark using sodium bicarbonate and their novel use in yarns for superior UV protection and antibacterial performance. *Ind. Crops Prod.* 164, 113387. <https://doi.org/10.1016/j.indcrop.2021.113387>.
- Dulie, N.W., Woldeyes, B., Demssah, H.D., Jabasingh, A.S., 2021. An insight into the valorization of hemicellulose fraction of biomass into furfural: catalytic conversion and product separation. *Waste Biomass Valorization* 12, 531–552. <https://doi.org/10.1007/s12649-020-00946-1>.
- Elli, E.F., Sentelhas, P.C., Bender, F.D., 2020. Impacts and uncertainties of climate change projections on *Eucalyptus* plantations productivity across Brazil. *For. Ecol. Manage.* 474, 118365. <https://doi.org/10.1016/j.foreco.2020.118365>.
- Fernández, K., Kappes, T., González, N., Gutiérrez, C., 2019. Influence of tree height on the hydrophilic and lipophilic composition of bark extracts from *Eucalyptus globulus* and *Eucalyptus nitens*. *Holzforchung* 73, 705–713. <https://doi.org/10.1515/hf-2018-0243>.
- Grootemaat, S., Wright, I.J., van Bodegom, P.M., Cornelissen, J.H.C., Shaw, V., 2017. Bark traits, decomposition and flammability of Australian forest trees. *Aust. J. Bot.* 65, 327–338. <https://doi.org/10.1071/BT16258>.
- Johansson, L.-S., Campbell, J., Koljonen, K., Kleen, M., Buchert, J., 2004. On surface distributions in natural cellulosic fibres. *Surf. Interface Anal.* 36, 706–710. <https://doi.org/10.1002/sia.1741>.
- Jorge, F., Quilhó, T., Pereira, H., 2000. Variability of fibre length in wood and bark in *Eucalyptus globulus*. *IAWA J.* 21, 41–48. <https://doi.org/10.1163/22941932-90000235>.
- Karakoç, A., Rastogi, V.K., Isoaho, T., Tardy, B., Paltakari, J., Rojas, O.J., 2020. Comparative screening of the structural and thermomechanical properties of FDM filaments comprising thermoplastics loaded with cellulose, carbon and glass fibers. *Materials* 13, 422. <https://doi.org/10.3390/ma13020422>.
- Kono, H., Yunoki, S., Shikano, T., Fujiwara, M., Erata, T., Takai, M., 2002. CP/MAS ¹³C NMR study of cellulose and cellulose derivatives. 1. Complete assignment of the CP/MAS ¹³C NMR spectrum of the native cellulose. *J. Am. Chem. Soc.* 124, 7506–7511. <https://doi.org/10.1021/ja010704o>.
- Ku, H., Wang, H., Pattarachaiyakoop, N., Trada, M., 2011. A review on the tensile properties of natural fiber reinforced polymer composites. *Compos. Part B Eng.* 42, 856–873. <https://doi.org/10.1016/j.compositesb.2011.01.010>.
- Li, L., Zhou, Y., Cheng, X., Sun, J., Marita, J.M., Ralph, J., Chiang, V.L., 2003. Combinatorial modification of multiple lignin traits in trees through multigene cotransformation. *Proc. Natl. Acad. Sci. U. S. A.* 100, 4939–4944. <https://doi.org/10.1073/pnas.0831166100>.
- Lima, M.A., Lavorente, G.B., da Silva, H.K., Bragatto, J., Rezende, C.A., Bernardinelli, O. D., deAzevedo, E.R., Gomez, L.D., McQueen-Mason, S.J., Labate, C.A., Polikarpov, I., 2013. Effects of pretreatment on morphology, chemical composition and enzymatic digestibility of eucalyptus bark: a potentially valuable source of fermentable sugars for biofuel production – part 1. *Biotechnol. Biofuels* 6, 75. <https://doi.org/10.1186/1754-6834-6-75>.
- Mazzanti, V., Pariante, R., Bonanno, A., Ruiz de Ballesteros, O., Mollica, F., Filippone, G., 2019. Reinforcing mechanisms of natural fibers in green composites: role of fibers morphology in a PLA/hemp model system. *Compos. Sci. Technol.* 180, 51–59. <https://doi.org/10.1016/j.compscitech.2019.05.015>.
- Miranda, I., Gominho, J., Pereira, H., 2012. Incorporation of bark and tops in *Eucalyptus globulus* wood pulping. *BioResources* 7, 4350–4361. <https://doi.org/10.15376/BIORES.7.3.4350-4361>.
- Neis, F.A., de Costa, F., de Araújo, A.T., Fett, J.P., Fett-Neto, A.G., 2019. Multiple industrial uses of non-wood pine products. *Ind. Crops Prod.* 130, 248–258. <https://doi.org/10.1016/j.indcrop.2018.12.088>.
- Neiva, D.M., Rencoret, J., Marques, G., Gutiérrez, A., Gominho, J., Pereira, H., del Río, J. C., 2020. Lignin from tree barks: chemical structure and valorization. *ChemSusChem* 13, 4537–4547. <https://doi.org/10.1002/cssc.202000431>.
- Normand, M.L., Moriana, R., Ek, M., 2014. The bark biorefinery: a side-stream of the forest industry converted into nanocomposites with high oxygen-barrier properties. *Cellulose* 21, 4583–4594. <https://doi.org/10.1007/s10570-014-0423-z>.
- Ouajai, S., Shanks, R.A., 2009. Biocomposites of cellulose acetate butyrate with modified hemp cellulose fibres. *Macromol. Mater. Eng.* 294, 213–221. <https://doi.org/10.1002/mame.200800266>.
- Pan, M., Lei, Q., Zhang, H., 2020. Prediction and confirmation of active ingredients in *Eucalyptus globulus* Labill leaves. *Ind. Crops Prod.* 154, 112631. <https://doi.org/10.1016/j.indcrop.2020.112631>.
- Park, M.G., Choi, J., Hong, Y.S., Park, C.G., Kim, B.G., Lee, S.Y., Lim, H.J., Mo, H., Lim, E., Cha, W., 2020. Negative effect of methyl bromide fumigation work on the central nervous system. *PLoS One* 15, e0236694. <https://doi.org/10.1371/journal.pone.0236694>.
- Pickering, K.L., Aruan Efendy, M.G., Le, T.M., 2016. A review of recent developments in natural fibre composites and their mechanical performance. *Compos. Part A* 83, 98–112. <https://doi.org/10.1016/j.compositesa.2015.08.038>.
- Quilhó, T., Pereira, H., 2001. Within and between-tree variation of bark content and wood density of *Eucalyptus globulus* in commercial plantations. *IAWA J.* 22, 255–265. <https://doi.org/10.1163/22941932-90000283>.
- Rencoret, J., Gutiérrez, A., Nieto, L., Jiménez-Barbero, J., Paulds, C.B., Kim, H., Ralph, J., Martínez, Á.T., del Río, J.C., 2011. Lignin composition and structure in young versus

- adult *Eucalyptus globulus* plants. *Plant Physiol.* 155, 667–682. <https://doi.org/10.1104/pp.110.167254>.
- Saha, P., Chowdhury, S., Roy, D., Adhikari, B., Kim, J.K., Thomas, S., 2016. A brief review on the chemical modifications of lignocellulosic fibers for durable engineering composites. *Polym. Bull.* 73, 587–620. <https://doi.org/10.1007/s00289-015-1489-y>.
- Sajaniemi, V., Karakoç, A., Paltakari, J., 2019. Mechanical and thermal behavior of natural fiber-polymer composites without compatibilizers. *Res. Eng. Struct. Mater.* 6, 63–73. <https://doi.org/10.17515/resm2019.124ma0308>.
- Shimizu, S., Yokoyama, T., Akiyama, T., Matsumoto, Y., 2012. Reactivity of lignin with different composition of aromatic Syringyl/Guaiacyl structures and Erythro/Threo side chain structures in β -O-4 type during alkaline delignification: As a basis for the different degradability of hardwood and softwood lignin. *J. Agric. Food Chem.* 60, 6471–6476. <https://doi.org/10.1021/jf301329v>.
- Sluiter, J.B., Ruiz, R.O., Scarlata, C.J., Sluiter, A.D., Templeton, D.W., 2010. Compositional analysis of lignocellulosic feedstocks. 1. Review and description of methods. *J. Agric. Food Chem.* 58, 9043–9053. <https://doi.org/10.1021/jf1008023>.
- Soares, B., da Costa Lopes, A.M., Silvestre, A.J.D., Rodrigues Pinto, P.C., Freire, C.S.R., Coutinho, J.A.P., 2021. Wood delignification with aqueous solutions of deep eutectic solvents. *Ind. Crops Prod.* 160, 113128 <https://doi.org/10.1016/j.indcrop.2020.113128>.
- Vázquez, G., Fontenla, E., Santos, J., Freire, M.S., González-Álvarez, J., Antorrena, G., 2008. Antioxidant activity and phenolic content of chestnut (*Castanea sativa*) shell and eucalyptus (*Eucalyptus globulus*) bark extracts. *Ind. Crops Prod.* 28, 279–285. <https://doi.org/10.1016/j.indcrop.2008.03.003>.
- Vázquez, G., Santos, J., Freire, M.S., Antorrena, G., González-Álvarez, J., 2012. Extraction of antioxidants from eucalyptus (*Eucalyptus globulus*) bark. *Wood Sci. Technol.* 46, 443–457. <https://doi.org/10.1007/s00226-011-0418-y>.
- Wibowo, A.C., Mohanty, A.K., Misra, M., Drzal, L.T., 2004. Chopped industrial hemp Fiber reinforced cellulosic plastic biocomposites: thermomechanical and morphological properties. *Ind. Eng. Chem. Res.* 43, 4883–4888. <https://doi.org/10.1021/ie030873c>.
- Xie, Y., Arnold, R.J., Wu, Z.H., Chen, S., Du, A., Luo, J., 2017. Advances in eucalypt research in China. *Front. Agric. Sci. Eng.* 4, 380–390. <https://doi.org/10.15302/J-FASE-2017171>.
- Yong, W.T.L., Ades, P.K., Goodger, J.Q.D., Bossinger, G., Runa, F.A., Sandhu, K.S., Tibbits, J.F.G., 2019. Using essential oil composition to discriminate between myrtle rust phenotypes in *Eucalyptus globulus* and *Eucalyptus obliqua*. *Ind. Crops Prod.* 140, 111595 <https://doi.org/10.1016/j.indcrop.2019.111595>.